Purifying Photon Indistinguishability through Quantum Interference

Carlos F. D. Faurby,[1,*] Lorenzo Carosini,[2,3,*] Huan Cao,[2,3,‡] Patrik I. Sund,[1] Lena M. Hansen,[2,3] Francesco Giorgino,[2,3] Andrew B. Villadsen,[1] Stefan N. van den Hoven,[4] Peter Lodahl,[1,5] Stefano Paesani,[1,5,†] Juan C. Loredo,[2,3] and Philip Walther[2,3,6,7]

[1]*Center for Hybrid Quantum Networks (Hy-Q), Niels Bohr Institute, University of Copenhagen, Blegdamsvej 17, Copenhagen 2100, Denmark*

[2]*University of Vienna, Faculty of Physics, Vienna Center for Quantum Science and Technology (VCQ), 1090 Vienna, Austria*

[3]*Christian Doppler Laboratory for Photonic Quantum Computer, Faculty of Physics, University of Vienna, 1090 Vienna, Austria*

[4]*MESA+ Institute for Nanotechnology, University of Twente, 7500AE Enschede, The Netherlands*

[5]*NNF Quantum Computing Programme, Niels Bohr Institute, University of Copenhagen, Blegdamsvej 17, Copenhagen 2100, Denmark*

[6]*University of Vienna, Research Network for Quantum Aspects of Space Time (TURIS), 1090 Vienna, Austria*

[7]*Institute for Quantum Optics and Quantum Information (IQOQI) Vienna, Austrian Academy of Sciences, Vienna, Austria*

(Received 21 March 2024; revised 8 May 2024; accepted 17 June 2024; published 18 July 2024)

Indistinguishability between photons is a key requirement for scalable photonic quantum technologies. We experimentally demonstrate that partly distinguishable single photons can be purified to reach near-unity indistinguishability by the process of quantum interference with ancillary photons followed by heralded detection of a subset of them. We report on the indistinguishability of the purified photons by interfering two purified photons and show improvements in the photon indistinguishability of 2.774(3)% in the low-noise regime, and as high as 10.2(5)% in the high-noise regime.

DOI: 10.1103/PhysRevLett.133.033604

The generation of pure single photons is a fundamental requirement for emergent technologies in photonic quantum communication and quantum information processing [1–3]. Deterministic single-photon sources utilizing two-level emitters offer a pathway for on-demand photon generation in multiphoton applications. They have been realized in various platforms, such as color centers in diamonds [4,5], organic molecules [6], trapped atoms [7], and quantum dots [8]. One of the key requirements for photon sources is the capability to generate highly indistinguishable photons [9] in order to realize multiphoton interference—a core process in photonic quantum technologies [10]. Epitaxially grown quantum dots (QD) can generate highly indistinguishable photons due to the ability to precisely engineer their semiconductor environment [11–13], and have recently enabled quantum interference experiments with an increasing number of photons [14–18]. Nonetheless, partial distinguishability remains a central noise mechanism that can pose challenges in the development of emitter-based photonic systems at the scale required in practical applications [19].

In solid-state quantum emitters, photon distinguishability arises from either fast (compared to the photon lifetime) physical processes such as pure dephasing due to interactions with phonons in the environment [see Fig. 1(a)], and slow processes (i.e., slower than the photon lifetime) such as spectral diffusion due to interactions with charges and polarization drifts [11,20]. The standard approach to mitigating such noise contributions has so far been to reduce the temperature in order to reduce the number of phonons, develop ultra-low-noise chip devices with very low electrical noise, and to reduce the emission lifetime (via the Purcell effect) in order to reduce the interaction time with the acoustic phonon modes [20]. Recent works have proposed a different mitigation strategy by using linear optical circuits and ancillary photons to purify single photons once they have been emitted [21,22]. Purification is a well-known concept in quantum information processing; it consists of consuming multiple copies of noisy quantum states to obtain a single output state where the noise is suppressed [23]. Its applications include the purification of entanglement [23,24] and of "magic states" for universal fault-tolerant quantum computation [25]. Sparrow and Marshall have adapted this concept to purify single indistinguishable photons by processing multiple partially distinguishable and unentangled photons through quantum interference in linear-optical circuits [21,22].

In this work, we report the experimental demonstration of linear-optical purification of photon indistinguishability. We use a solid-state QD as a quantum emitter and tune both the fast and slow contributions in order to control the partial distinguishability of the emitted photons. The generated photons are subsequently processed with a fiber-based linear-optical interferometer to purify single

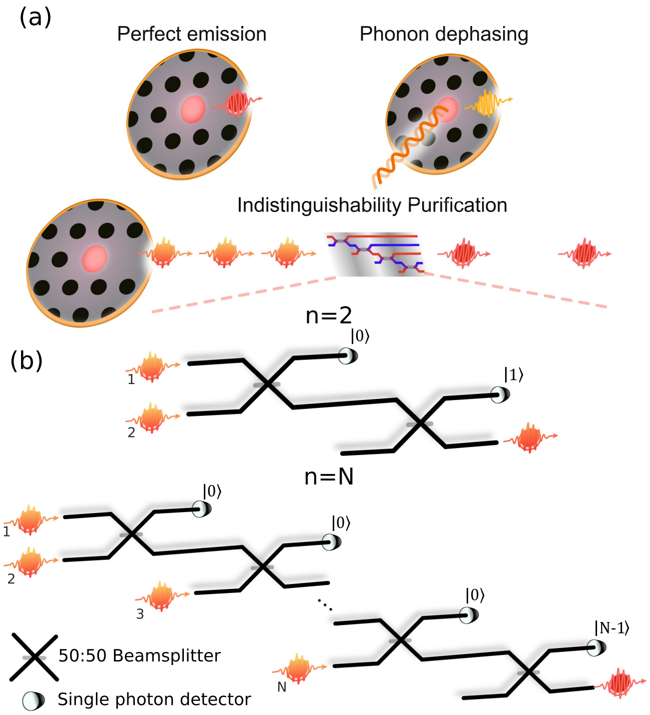

FIG. 1. Purification schemes. (a) Dephasing processes in quantum dots add distinguishability to the emitted photons. (b) Linear-optical circuits, based on cascaded Hong-Ou-Mandel-type quantum interferometers, for purifying indistinguishable photons considered in this work for $n = 2$ photons (top) and an arbitrary photon number $n = N$ (bottom).

indistinguishable photons. The indistinguishability of the purified photons is analyzed by simultaneously implementing two copies of the purification circuit and performing quantum interference between the purified output photons. By tuning the noise contributions in the QD system, we test the purification protocol both where the dominant distinguishability contributions are fast processes, as well as cases where slow noises are dominant. In all cases, the results show significant improvement of the indistinguishability of the purified photons compared to the initial ones, showing the strong potential of this approach for developing ultra-low-noise photonic quantum technologies.

Indistinguishability purification circuits.—The protocols we experimentally investigate exploit the difference in the statistics of indistinguishable and distinguishable photons interfering on a beam splitter to amplify the indistinguishable components of the quantum state. In particular, we implement the linear-optical purification circuits schematized in Fig. 1(b), which was originally proposed by Sparrow [21] and further refined by Marshall [22]. It works as follows: according to the Hong-Ou-Mandel (HOM) effect, indistinguishable photons bunch when interfering on a balanced beam splitter (BS), while distinguishable photons only do so half of the time [26]. Therefore by heralding on the absence of the detection of a photon in one output port of the beam splitter (indicating that there are two bunched photons in the other mode), the amplitude of the indistinguishable component of the photons state is thus enhanced as the distinguishable part is less likely to provide such a measurement event. A purified single photon can subsequently be extracted from the two bunched photons in a heralded manner by probabilistically splitting them with an additional BS and detecting a single photon in one of the output arms. This constitutes the $n = 2$ case illustrated in Fig. 1(b), where two photons are used to create an output photon with improved indistinguishability. The method can be generalized by repeated HOM interferences followed by zero-photon detection in order to further purify the indistinguishable component of the state, as also illustrated in Fig. 1(b) corresponding to the case where N single photons are applied. In this scheme, the improvement comes at the expense of a reduced success probability according to [21]

$$P_{\text{success}} = \frac{(n-1)!}{2\sum_{i=2}^{n} i} \cdot \frac{n^2}{2^n}. \tag{1}$$

The success probability is 25% for the $n = 2$ case and decreases exponentially for higher n.

This decrease can be mitigated by changing the reflectivity of the final beam splitter, and further optimized by using different interferometers with different heralding patterns [22]. Moreover, because the detection also provides a heralding of success, multiplexing techniques can then be used to turn the heralded probabilistic process into near deterministic [27].

Experimental setup.—A schematic of the full experimental setup, which implements two copies of the $n = 2$ purification circuits and performs quantum interference between the two purified outputs, is shown in Fig. 2. Deterministic single-photon generation is achieved from a neutral exciton of an InAs QD embedded in photonic crystal waveguide (PCW), detailed in the bottom left inset of Fig. 2. The QD is pumped resonantly with a pulsed laser, spectrally shaped with a home-built folded 4-f system, to set a bandwidth of ~90 pm and match the QD wavelength $\lambda = 938.4$ nm. Electrical tuning of the QD, facilitated by low-noise electrical contacts, stabilizes the charge state, ensuring emission on the desired transition and minimizing spectral diffusion due to residual charge noise [12,28]. The single photons are emitted in the PCW and fiber coupled via a shallow-edged grating and a cryocompatible objective lens. An etalon with a bandwidth of 32 GHz can be employed as a frequency filter to optimize the indistinguishability of emitted photons by removing the undesired phonon-induced spectral sideband. Pumping the QD with resonant π pulses at a repetition rate of 80 MHz yields single photons at a measured rate of 16.1 MHz (with an 85% efficient detection system), corresponding to a 23.7% fiber-coupled efficiency of the single-photon source, and purity of $1 - g^{(2)}(0) = (97.21 \pm 0.01)\%$. The photon stream is then converted into four streams of simultaneous

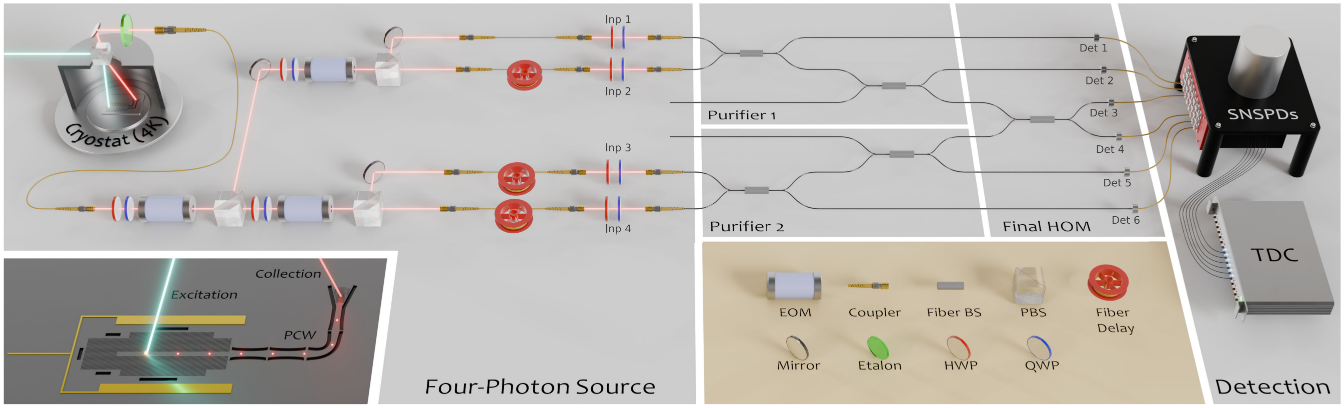

FIG. 2. Experiment schematic. The single-photon source (inset) is an InAs QD coupled to a GaAs PCW, gated via metal electrical contacts (depicted in gold), kept at 4 K inside a cryostat. An etalon serves as a frequency filter, eliminating phonon side bands to maximize photon indistinguishability. The emitted single-photon stream is routed into four spatial modes through a free-space demultiplexer, generating sets of four simultaneous input photons. Fiber-based temporal delays precede a final free-space setup, ensuring precise polarization control and enabling artificial delays before the purification stages. (Center) Two copies of the indistinguishability purification circuit are implemented through fiber beam splitter (BS), and the outputs interfere at a final BS to test the indistinguishability of purified photons. (Right) Output configurations are measured through six superconducting nanowire single-photon detectors (SNSPDs) and a time-to-digital converter (TDC) to process their time tags.

photons in different spatial modes through a time-to-space demultiplexing module. As shown in Fig. 2, it consists of three resonantly enhanced electro-optic modulators (EOMs) and polarizing beam splitters (PBSs) arranged in a treelike structure [29,34] to route the photons in four different output modes and with different fiber lengths to compensate for the temporal delays. At this stage, we detect four-photon coincidences at a rate of 3.2 kHz. An additional free-space coupling is introduced before feeding into the fiber-based HOM interferometers to precisely control the polarization of photons via half- and quarter-wave plates (HWP and QWP, respectively).

The purification circuits are implemented with optical fibers and involves two fiber beam splitters for each copy of the scheme, with the purified photons interfering in a final BS. We characterized the optical losses induced by the purification setup to be of 1 dB. These are mainly due to fiber connectors between the beam splitters. Because the overall circuit is based on cascaded HOM interferometers, which are phase insensitive, no active phase stabilization is required. The photons are finally directed to six superconducting-nanowire single-photon detectors (SNSPDs, average 85% system efficiency) to measure the output configurations.

Results.—To analyze the improvement in indistinguishability induced by the purification, we first assessed the raw HOM visibility by interfering only two demultiplexed photons (inputs 1 and 4 in Fig. 2) by blocking inputs 2 and 3. Inputs 2 and 3 are then unblocked to implement the full circuit to test quantum interference between purified photons and extract their purified indistinguishability (see Supplemental Material [30] for details).

The purification protocol was tested in different experimental configurations of the QD, each with a different value of partial distinguishability between the emitted photons. The data from each configuration are shown in Fig. 3. In the first configuration ["no etalon" label in Fig. 3(b)], we test the protocol in a high-noise scenario by removing the etalon filter after the QD, which results in higher distinguishability due to the presence of incoherent spectral sidebands. This is indeed manifested in a measured low raw HOM visibility of $V_0 = 0.5829(1)$, as depicted in Fig. 3(a)(lower). When the purification protocol is implemented, the visibility of HOM interference between the purified photons was increased to $V_f = 0.685(5)$ as depicted in Fig. 3(a)(upper), marking a significant improvement of 10.2(5)%. The purple curve is both narrower and has a lower maximum than the red curve, suggesting that both the dynamics and the amplitude of the distinguishable components are altered. The width of the peak nonetheless only changes due to the lower heralding probability of photons far away from the center position, as the effect can also be seen on the side peaks. It can thus not be concluded that the purified photons have different properties than the raw ones, except for a lower distinguishable component.

In a second QD configuration ["optimal" label in Fig. 3(b)], the etalon was added to test the protocol in a low-noise environment where most phonon-induced noise is filtered out. The initial raw HOM visibility was measured to be $V_0 = 0.9050(1)$, which is then improved to $V_f = 0.9327(1)$ using the purified photons. As discussed in the Supplemental Material [30], we estimate that in this case the remaining noise contributions limiting the visibility are dominated by spurious multiphoton terms arising by the finite $g^{(2)}(0)$ of the QD, while contributions due to partial distinguishability is mostly removed via the purification.

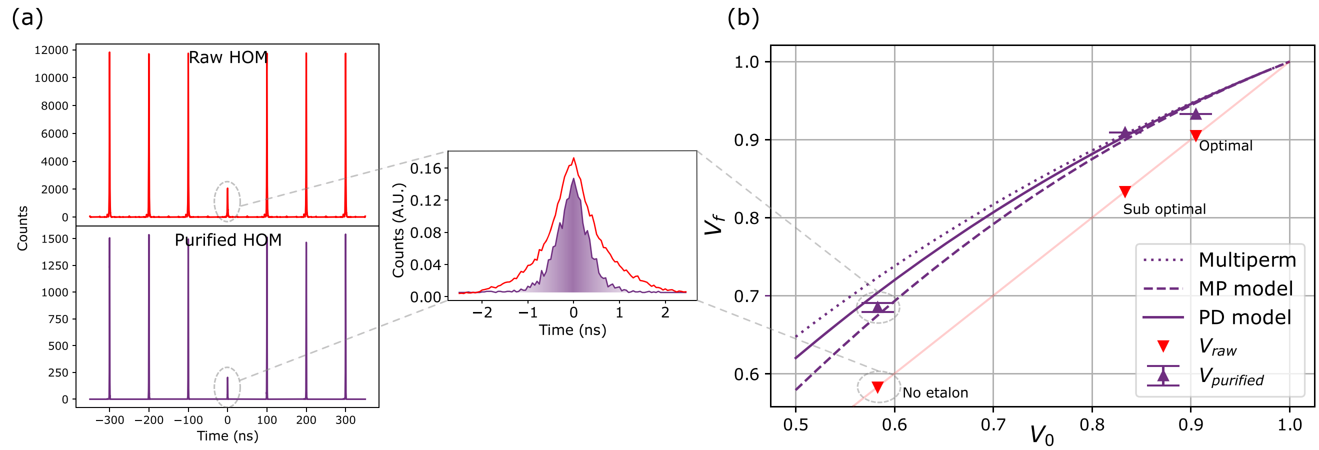

FIG. 3. Purification results for fast noise processes. (a) Two-photon correlation measurement results for HOM experiments with raw (top) and purified (bottom) photons. (Inset) Normalized central peaks for both cases, showing an improved suppression for the purified (purple) case. (b) Obtained improvements in visibility for three configurations of the QD source with different noise levels. The curves show the theoretical estimates for different noise models, as described in the main text. The error bars (only shown when exceeding the size of the markers) are calculated via Monte Carlo error propagation assuming Poissonian photon statistics.

We tested one additional scenario ["suboptimal" label in Fig. 3(b)], where we keep the etalon but intentionally detune the voltage applied to the QD from its optimal value. Applying a voltage that is closer to the edge of the charge plateau increases the probability of cotunneling of carriers to the contacts. This experimental condition induced a slight reduction in raw HOM visibility to $V_0 = 0.8332(1)$, which is then enhanced to visibility of $V_f = 0.9090(5)$ through purification.

The data histograms which are the base for the suboptimal and optimal configuration results are shown in the Supplemental Material [30].

In Fig. 3 we also plot the theoretical estimations of the indistinguishability for the purified photons as a function of the raw visibilities, and used in addition three different models for predicting the partial distinguishability of the photons. The first model, which we call the "multipermanent model" [dotted curve in Fig. 3(b)], assumes a constant state overlap and orthogonality between the distinguishable components of each photon, as outlined in [35]. A second considered model, based on the minimum purity model [MP, dashed curve in Fig. 3(b)] of Ref. [21], assumes that the internal degrees of freedom of all photons are in the same mixed state whose finite purity is the cause for distinguishability. Finally, we introduce a physically motivated model, denoted as the pure-dephasing model [PD, solid curve in Fig. 3(b)], that considers the noise processes inherent in a QD environment and incorporates higher-order indistinguishability instances (e.g., 3 and 4-photon contributions). The theoretical curves give slightly different expected improvements but are in good agreement with the observed measurements. For a comprehensive explanation and discussion of these diverse models, please refer to the Supplemental Material [30].

After demonstrating successful purification for the case of a fast physical process, in particular phonon-induced dephasing, we test the purification protocol in the presence of slow errors as well. In this case, we deliberately altered the

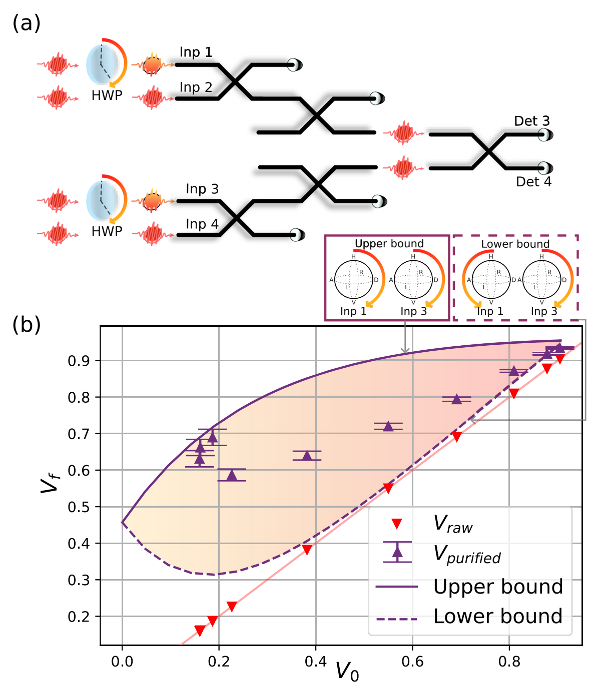

FIG. 4. Purification results for slow noise processes. (a) Purification in the presence of polarization-induced distinguishability contributions implemented by rotating the HWP of inputs 1 and 3. (b) Experimental purified indistinguishabilities (purple markers) for various raw HOM visibilities (red markers). The theoretical upper and lower bounds are the expected improved values in the cases where the polarizations of inputs 1 and 3 are rotated in the same or opposite directions, respectively.

polarization of one input photon per purifier, as illustrated in Fig. 4(a), and again evaluated the HOM visibility before and after purification. The results, shown in Fig. 4(b), compare our experimental data (in purple) with a simulation illustrating the application of the purification protocol to photons with different polarizations. The polarization of the photons after going through multiple fiber BSs is transformed in randomized by temperature drift and bending of the fibers, and thus setting for a specific transformation is not attempted. The upper bound comes when the photons' polarization is rotated in the same direction of the Bloch sphere, while the lower bound comes when they are rotated in opposite directions. Both cases are illustrated in the upper side of Fig. 4(b), and the associated curves are plotted together with the measured raw and purified HOM visibilities. Representative histograms used to generate three of the data-points from the figure are shown in the Supplemental Material [30]. The observed data again show significant improvements in the indistinguishability and compatible with the theoretical bounds described above, demonstrating the realization of a successful purification protocol for both slow and fast noise contributions.

It is important to mention that when comparing success probabilities of individual instances, spectral filtering can give a better performance than purification. However, there are essential differences between the two approaches that result in different advantages. First, filtering is a loss process. Its probabilistic nature is fundamental and there is no way to recover it as a near-deterministic operation. In contrast, our approach can be implemented through multiplexing of heralded events. Secondly, spectral filtering is effective in reducing distinguishability for certain noise sources (e.g. spectral detuning, phonon sidebands, spectral correlations in spontaneous photon sources) but is ineffective in correcting most incoherent processes, such as pure dephasing. Remarkably our scheme is not facing this limitation, making it operationally distinct from spectral filtering by being able to purify also incoherent processes.

Conclusions.—We have demonstrated a new type of purification process in quantum optical systems: the purification of partially distinguishable photons through quantum interference. Significant indistinguishability improvements are observed already for a small purification circuit involving $n = 2$ input photons. We remark that the demonstrated capability to mitigate both fast and slow noise processes is in strong contrast to previous noise mitigation techniques, e.g., environment monitoring in solid-state emitters [36] and time-resolved measurement techniques [37,38], which only work for slow noises (e.g., spectral diffusion and frequency mismatch in the above examples, respectively). The versatility of the approach highlights its relevance for any quantum photonic platform. In fact, the same approach can be straightforwardly used to purify photons also from other types of photon emitters, including atoms [7] and heralded photon sources [39].

The purification protocols come at the cost of additional ancillary photons and, when relevant, multiplexing circuits to turn their probabilistic nature into near deterministic. These are functionalities already required in photonic quantum computing architectures based on single photons [40]. The hardware overhead of the purification protocols is anyway likely largely dominated in practice by the overheads required in other parts of the architecture, such as in photonic entanglement generation circuits [41] and quantum error correction [42,43]. Furthermore, the purification circuits implemented here can be significantly improved by modulating the reflectivities of the BSs or using discrete Fourier-transform interferometers [21,22], enabling significantly higher success probabilities and indistinguishability improvements. Our study provides new and versatile experimental tools to purify photons and mitigate fundamental noise processes that ultimately may limit the scaling-up of photonic quantum technologies based on quantum emitters.

We thank Alex E. Jones for fruitful discussions. We acknowledge funding from the Danish National Research Foundation (Center of Excellence "Hy-Q," Grant No. DNRF139), the Novo Nordisk Foundation (Challenge project "Solid-Q"), the European Union's Horizon 2020 research and innovation program under Grant Agreement No. 820445 (project name Quantum Internet Alliance), No. 899368 (EPIQUS), the Marie Skłodowska-Curie grant agreement No. 956071 (AppQInfo), and the European Union's Horizon Europe research and innovation program under Grant Agreement No. 101135288 (EPIQUE) and No. 101017733 (QuantERA II, programme, project PhoMemtor). Views and opinions expressed are however those of the author(s) only and do not necessarily reflect those of the European Union or the European Research Council Executive Agency. This research was funded in whole or in part by the Austrian Science Fund (FWF) [10.55776/COE1] (Quantum Science Austria), [10.55776/F71] (BeyondC) and [10.55776/FG5] (Research Group 5). The financial support from the Austrian Federal Ministry of Labour and Economy, the National Foundation for Research, Technology and Development and the Christian Doppler Research Association is gratefully acknowledged. S. P. acknowledges financial support from the European Union's Horizon 2020 Marie Skłodowska-Curie Grant No. 101063763, from the Villum Fonden research Grants No. VIL50326 and No. VIL60743, and from the NNF Quantum Computing Programme. P. L. is the founder of the company Sparrow Quantum.

*These authors contributed equally to this letter.
†Contact author: stefano.paesani@nbi.ku.dk
‡Contact author: huan.cao@univie.ac.at

[1] S. Slussarenko and G. J. Pryde, Photonic quantum information processing: A concise review, Appl. Phys. Rev. **6** (2019).

[2] J. L. O'brien, A. Furusawa, and J. Vučković, Photonic quantum technologies, Nat. Photonics **3**, 687 (2009).

[3] W. Luo, L. Cao, Y. Shi, L. Wan, H. Zhang, S. Li, G. Chen, Y. Li, S. Li, Y. Wang *et al.*, Recent progress in quantum photonic chips for quantum communication and internet, Light Sci. Appl. **12**, 175 (2023).

[4] M. W. Doherty, N. B. Manson, P. Delaney, F. Jelezko, J. Wrachtrup, and L. C. Hollenberg, The nitrogen-vacancy colour centre in diamond, Phys. Rep. **528**, 1 (2013).

[5] G. Zhang, Y. Cheng, J.-P. Chou, and A. Gali, Material platforms for defect qubits and single-photon emitters, Appl. Phys. Rev. **7**, 031308 (2020).

[6] G. Murtaza, M. Colautti, M. Hilke, P. Lombardi, F. S. Cataliotti, A. Zavatta, D. Bacco, and C. Toninelli, Efficient room-temperature molecular single-photon sources for quantum key distribution, Opt. Express **31**, 9437 (2023).

[7] M. Mücke, J. Bochmann, C. Hahn, A. Neuzner, C. Nölleke, A. Reiserer, G. Rempe, and S. Ritter, Generation of single photons from an atom-cavity system, Phys. Rev. A **87**, 063805 (2013).

[8] P. Lodahl, S. Mahmoodian, and S. Stobbe, Interfacing single photons and single quantum dots with photonic nanostructures, Rev. Mod. Phys. **87**, 347 (2015).

[9] L. Mandel, Coherence and indistinguishability, Opt. Lett. **16**, 1882 (1991).

[10] J. L. O'brien, Optical quantum computing, Science **318**, 1567 (2007).

[11] A. V. Kuhlmann, J. Houel, A. Ludwig, L. Greuter, D. Reuter, A. D. Wieck, M. Poggio, and R. J. Warburton, Charge noise and spin noise in a semiconductor quantum device, Nat. Phys. **9**, 570 (2013).

[12] R. Uppu, F. T. Pedersen, Y. Wang, C. T. Olesen, C. Papon, X. Zhou, L. Midolo, S. Scholz, A. D. Wieck, A. Ludwig *et al.*, Scalable integrated single-photon source, Sci. Adv. **6**, eabc8268 (2020).

[13] X. Ding, Y. He, Z.-C. Duan, N. Gregersen, M.-C. Chen, S. Unsleber, S. Maier, C. Schneider, M. Kamp, S. Höfling *et al.*, On-demand single photons with high extraction efficiency and near-unity indistinguishability from a resonantly driven quantum dot in a micropillar, Phys. Rev. Lett. **116**, 020401 (2016).

[14] H. Wang, J. Qin, X. Ding, M.-C. Chen, S. Chen, X. You, Y.-M. He, X. Jiang, L. You, Z. Wang *et al.*, Boson sampling with 20 input photons and a 60-mode interferometer in a 1 0 14-dimensional hilbert space, Phys. Rev. Lett. **123**, 250503 (2019).

[15] S. Chen, L.-C. Peng, Y.-P. Guo, X.-M. Gu, X. Ding, R.-Z. Liu, J.-Y. Zhao, X. You, J. Qin, Y.-F. Wang, Y.-M. He, J. J. Renema, Y.-H. Huo, H. Wang, C.-Y. Lu, and J.-W. Pan, Heralded three-photon entanglement from a single-photon source on a photonic chip, Phys. Rev. Lett. **132**, 130603 (2024).

[16] P. I. Sund, E. Lomonte, S. Paesani, Y. Wang, J. Carolan, N. Bart, A. D. Wieck, A. Ludwig, L. Midolo, W. H. Pernice *et al.*, High-speed thin-film lithium niobate quantum processor driven by a solid-state quantum emitter, Sci. Adv. **9**, eadg7268 (2023).

[17] N. Maring *et al.*, A versatile single-photon-based quantum computing platform, Nat. Photonics **18**, 603 (2024).

[18] L. Carosini, V. Oddi, F. Giorgino, L. M. Hansen, B. Seron, S. Piacentini, T. Guggemos, I. Agresti, J. C. Loredo, and P. Walther, Programmable multiphoton quantum interference in a single spatial mode, Sci. Adv. **10**, eadj0993 (2024).

[19] P. I. Sund, R. Uppu, S. Paesani, and P. Lodahl, Hardware requirements for realizing a quantum advantage with deterministic single-photon sources, Phys. Rev. A **109**, 042613 (2024).

[20] P. Tighineanu, C. L. Dreeßen, C. Flindt, P. Lodahl, and A. S. Sørensen, Phonon decoherence of quantum dots in photonic structures: Broadening of the zero-phonon line and the role of dimensionality, Phys. Rev. Lett. **120**, 257401 (2018).

[21] C. Sparrow, Quantum interference in universal linear optical devices for quantum computation and simulation, Ph.D. thesis, Imperial College London, 2017.

[22] J. Marshall, Distillation of indistinguishable photons, Phys. Rev. Lett. **129**, 213601 (2022).

[23] C. H. Bennett, G. Brassard, S. Popescu, B. Schumacher, J. A. Smolin, and W. K. Wootters, Purification of noisy entanglement and faithful teleportation via noisy channels, Phys. Rev. Lett. **76**, 722 (1996).

[24] J.-W. Pan, S. Gasparoni, R. Ursin, G. Weihs, and A. Zeilinger, Experimental entanglement purification of arbitrary unknown states, Nature (London) **423**, 417 (2003).

[25] S. Bravyi and A. Kitaev, Universal quantum computation with ideal clifford gates and noisy ancillas, Phys. Rev. A **71**, 022316 (2005).

[26] C.-K. Hong, Z.-Y. Ou, and L. Mandel, Measurement of subpicosecond time intervals between two photons by interference, Phys. Rev. Lett. **59**, 2044 (1987).

[27] E. Meyer-Scott, C. Silberhorn, and A. Migdall, Single-photon sources: Approaching the ideal through multiplexing, Rev. Sci. Instrum. **91**, 041101 (2020).

[28] F. T. Pedersen, Y. Wang, C. T. Olesen, S. Scholz, A. D. Wieck, A. Ludwig, M. C. LObl, R. J. Warburton, L. Midolo, R. Uppu *et al.*, Near transform-limited quantum dot linewidths in a broadband photonic crystal waveguide, ACS Photonics **7**, 2343 (2020).

[29] F. Lenzini, B. Haylock, J. C. Loredo, R. A. Abrahao, N. A. Zakaria, S. Kasture, I. Sagnes, A. Lemaitre, H.-P. Phan, D. V. Dao *et al.*, Active demultiplexing of single photons from a solid-state source, Laser Photonics Rev. **11**, 1600297 (2017).

[30] See Supplemental Material at http://link.aps.org/supplemental/10.1103/PhysRevLett.133.033604 for a discussion of the models used, an analysis of the different sources of errors, a description of the data analysis methods, and supplementary data, which includes Refs. [31–33].

[31] S. Scheel, Permanents in linear optical networks, arXiv:quant-ph/0406127.

[32] E. M. González-Ruiz, S. K. Das, P. Lodahl, and A. S. Sørensen, Violation of Bell's inequality with quantum-dot single-photon sources, Phys. Rev. A **106**, 012222 (2022).

[33] M. Vyvlecka, L. Jehle, C. Nawrath, F. Giorgino, M. Bozzio, R. Sittig, M. Jetter, S. L. Portalupi, P. Michler, and P. Walther, Robust excitation of c-band quantum dots for quantum communication, Appl. Phys. Lett. **123** (2023).

[34] H. Cao, L. M. Hansen, F. Giorgino, L. Carosini, P. Zahálka, F. Zilk, J. C. Loredo, and P. Walther, Photonic source of

heralded greenberger-horne-zeilinger states, Phys. Rev. Lett. **132**, 130604 (2024).

[35] M. C. Tichy, Sampling of partially distinguishable bosons and the relation to the multidimensional permanent, Phys. Rev. A **91**, 022316 (2015).

[36] G. Éthier-Majcher, D. Gangloff, R. Stockill, E. Clarke, M. Hugues, C. Le Gall, and M. Atatüre, Improving a solid-state qubit through an engineered mesoscopic environment, Phys. Rev. Lett. **119**, 130503 (2017).

[37] T. Legero, T. Wilk, M. Hennrich, G. Rempe, and A. Kuhn, Quantum beat of two single photons, Phys. Rev. Lett. **93**, 070503 (2004).

[38] P. Yard, A. E. Jones, S. Paesani, A. Maïnos, J. F. F. Bulmer, and A. Laing, On-chip quantum information processing with distinguishable photons, Phys. Rev. Lett. **132**, 150602 (2024).

[39] M. Tanida, R. Okamoto, and S. Takeuchi, Highly indistinguishable heralded single-photon sources using parametric down conversion, Opt. Express **20**, 15275 (2012).

[40] D. E. Browne and T. Rudolph, Resource-efficient linear optical quantum computation, Phys. Rev. Lett. **95**, 010501 (2005).

[41] P. J. Shadbolt, M. R. Verde, A. Peruzzo, A. Politi, A. Laing, M. Lobino, J. C. Matthews, M. G. Thompson, and J. L. O'Brien, Generating, manipulating and measuring entanglement and mixture with a reconfigurable photonic circuit, Nat. Photonics **6**, 45 (2012).

[42] S. Bartolucci, P. Birchall, H. Bombin, H. Cable, C. Dawson, M. Gimeno-Segovia, E. Johnston, K. Kieling, N. Nickerson, M. Pant *et al.*, Fusion-based quantum computation, Nat. Commun. **14**, 912 (2023).

[43] S. Paesani and B. J. Brown, High-threshold quantum computing by fusing one-dimensional cluster states, Phys. Rev. Lett. **131**, 120603 (2023).